

Electronic Supplementary Information

**Ionic Liquid Functionalized 3D Mesoporous FDU-12 for
Effective SO₂ Capture**

Shuaiqi Gao, Pengling Zhang*, Zhenzhen Wang, Guokai Cui, Jikuan Qiu, and
Jianji Wang*

*Collaborative Innovation Center of Henan Province for Green Manufacturing of Fine
Chemicals, Key Laboratory of Green Chemical Media and Reactions, Ministry of Education,
School of Chemistry and Chemical Engineering, Henan Normal University, Xinxiang, Henan
453007, People's Republic of China*

*E-mail: zhangpengling@htu.edu.cn (P. Zhang),
jwang@htu.cn (J. Wang).*

Number of pages: 12

Number of Figures: 12

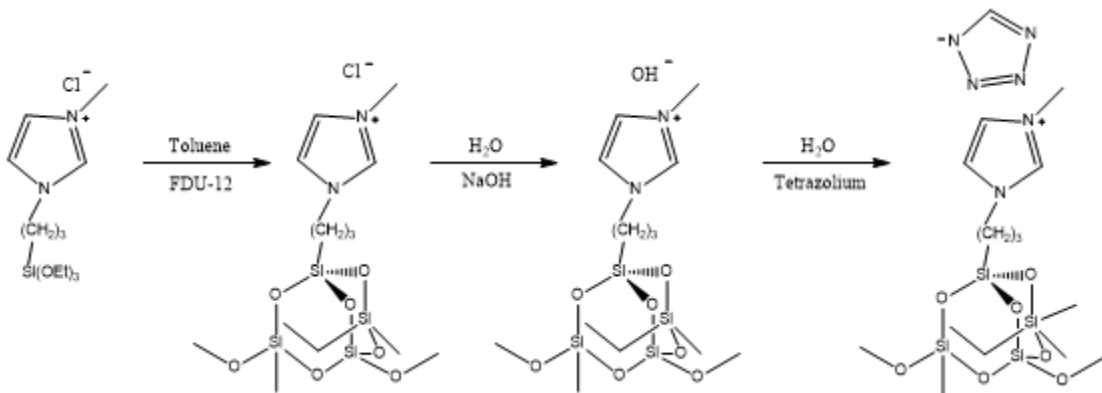
Number of Tables: 4

Table of Contents

1. ^1H NMR data of the IL.....	S3
2. Scheme S1. Schematic illumination of the IL grafting.....	S3
3. Tables S1-S4	
Table S1. The properties of porosity for neat FDU-12 samples synthesized at different temperatures.....	S3
Table S2. Elemental analysis results for the IL@FDU-12-1 samples prepared at different IL loadings.....	S4
Table S3. The properties of porosity and SO_2 adsorption capacity for IL@FDU-12-1, IL@FDU-12-2, IL@FDU-12-3 and IL@FDU-12-4 samples synthesized at $R=1.5$	S4
Table S4. The effect of water content on SO_2 capture by IL@FDU-12-1 sample prepared at $R=1.5$	S5
4. Figures S1-S12	
Figure S1. N_2 absorption isotherms (A) and BJH pore size distribution (B) for neat FDU-12 samples.....	S6
Figure S2. SAXS patterns for neat FDU-12 samples with different pore sizes.....	S7
Figure S3. The stability of mesoporous structure of FDU-12-1 sample.....	S7
Figure S4. TEM image of the neat FDU-12-1 sample.....	S8
Figure S5. SEM images and the corresponding EDS elemental mapping images of the IL-FDU-12-1 sample prepared at $R = 1.5$	S8
Figure S6. The effect of the grafted IL content on SO_2 absorption capacity.....	S9
Figure S7. SAXS patterns of the IL@FDU-12 samples prepared at $R = 1.5$	S9
Figure S8. N_2 adsorption isotherms (A) and pore size distribution (B) of the IL@FDU-12 samples prepared at $R = 1.5$	S10
Figure S9. The effect of partial pressure on SO_2 adsorption capacity.....	S10
Figure S10. FT-IR spectrum of FDU-12-1 and IL@FDU-12-1 synthesized at $R = 1.5$ before and after capture of SO_2	S11
Figure S11. FT-IR spectrum of neat IL before and after capture of SO_2	S11
Figure S12. CO_2 uptake by IL@-FDU-12-1 synthesized at $R = 1.5$	S12

¹H NMR data of the IL

[C₆Mim][Tetz]: ¹H NMR (D₂O): 0.75 (t, 3H, NC₅H₁₀CH₃), 1.16 (m, 6H, NC₂H₄(CH₂)₃), 1.74 (m, 2H, NCH₂CH₂), 3.76 (s, 3H, NCH₃), 4.02 (m, 2H, NCH₂), 7.29 (t, 1H, Im C5), 7.33(t, 1H, Im C4), 8.47 (s, 1H, Tetz C2), 8.55 (s, 1H, Im C2) ppm.



Scheme S1. Schematic illumination of the IL grafting.

Table S1. The properties of porosity for neat FDU-12 samples synthesized at different temperatures ^a

sample	T/°C	S _{BET} /m ² /g	V _t /cm ³ /g	D _c /nm	D _w /nm
FDU-12-1	14	651	0.74	17.5	3.8
FDU-12-2	20	741	0.69	12.3	3.8
FDU-12-3	25	602	0.65	12.5	3.8
FDU-12-4	35	630	0.68	7.8	3.8

^a S_{BET}, BET specific surface area; V_t, single-point pore volume; D_c, cage size calculated from the adsorption branch; D_w, entrance size calculated from the desorption branch.

Table S2. Elemental analysis results for the IL@FDU-12-1samples prepared at different IL loadings ^a

sample	N (wt %) ^b	C (wt %) ^b	Grafted IL content ^c (mmol/g)
<i>R</i> = 0.5	1.91	3.97	0.23
<i>R</i> = 1.0	2.76	6.26	0.33
<i>R</i> = 1.5	3.39	6.00	0.40
<i>R</i> = 3.0	4.37	8.35	0.52
<i>R</i> = 3.5	4.42	7.46	0.53
<i>R</i> = 4.0	1.25	4.04	0.15

^a *R* stands for the mass ratio of IL to FDU-12-1; ^b obtained from elemental analysis,

^c calculated from N content.

Table S3. The properties of porosity and SO₂ adsorption capacity for IL@FDU-12-1, IL@FDU-12-2, IL@FDU-12-3 and IL@FDU-12-4 samples synthesized at *R* =1.5

sample	S _{BET} ^a m ² /g	V _t / ^b cm ³ /g	D _c / ^c nm	D _w / ^d nm	SO ₂ uptake ^e (mmol/g)
IL@FDU-12-1	415	0.62	17.5	3.8	7.21
IL@FDU-12-2	332	0.41	12.3	3.8	6.49
IL@FDU-12-3	351	0.52	12.5	3.8	6.52
IL@FDU-12-4	391	0.51	7.8	3.8	6.11

^a S_{BET}, BET specific surface area; ^b V_t, single-point pore volume; ^c D_c, cage size calculated from the adsorption branch; ^d D_w, entrance size calculated from the desorption branch; ^e SO₂ adsorption capacity at 25°C and 1 bar.

Table S4. The effect of water content on SO₂ capacity by IL@FDU-12-1 sample prepared at $R = 1.5$ ^a

adsorbent	water loading ^b mmol/g	dry SO ₂ mmol/g	wet SO ₂ ^c mmol/g
FDU-12-1	1.73	5.01	5.21
IL@FDU-12-1	4.86	7.22	7.32

^a Performed at 25 °C and 1 bar for 90 min. ^b Relative humidity is 100%. ^c Does not include mass of loaded water.

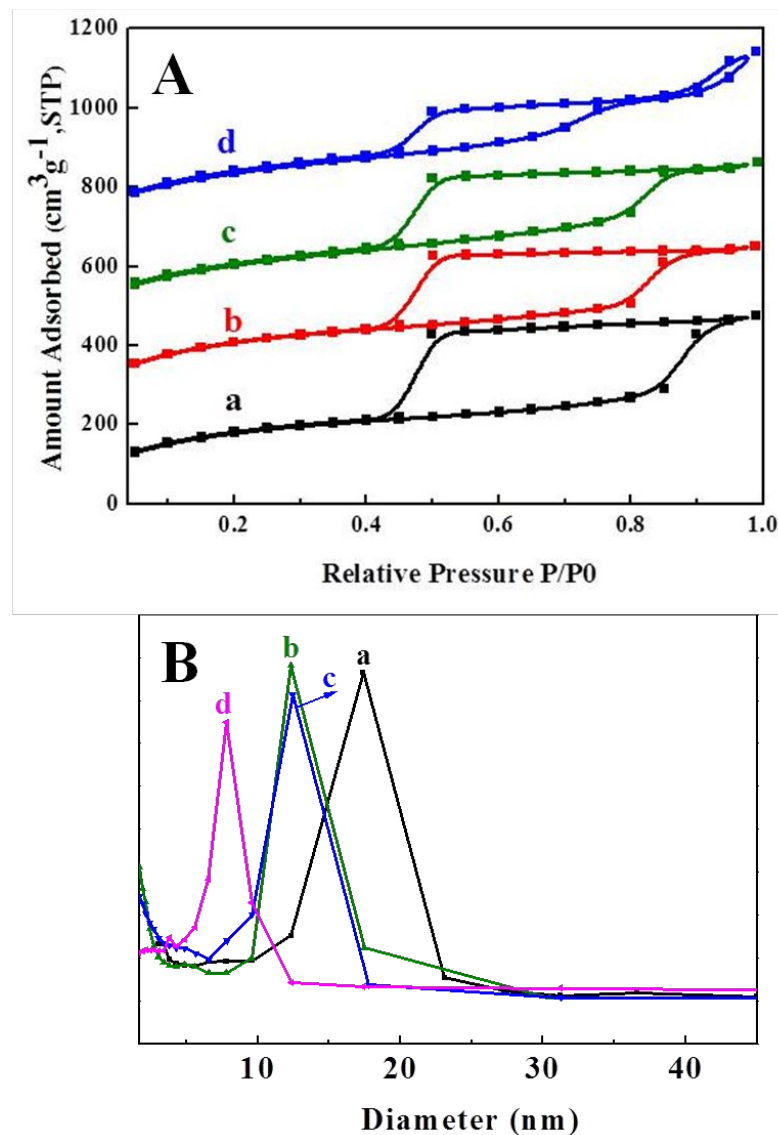


Figure S1. N₂ absorption isotherms (A) and BJH pore size distribution (B) for neat FDU-12 samples: (a) FDU-12-1, (b) FDU-12-2, (c) FDU-12-3, (d) FDU-12-4.

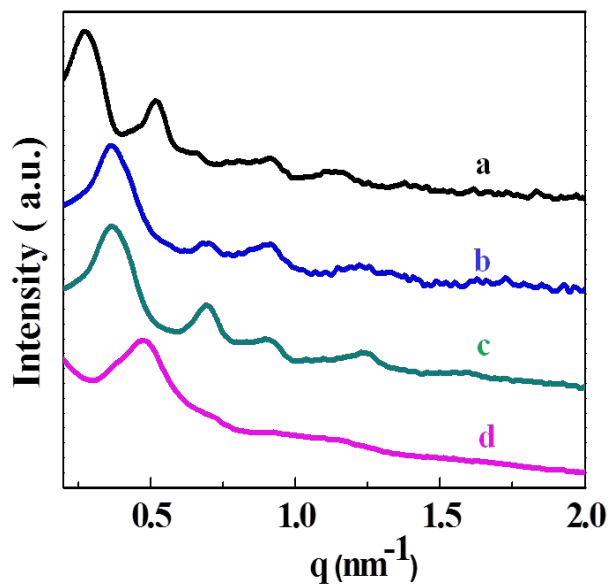


Figure S2. SAXS patterns for the neat FDU-12 samples with different pore sizes: (a) FDU-12-1, (b) FDU-12-2, (c) FDU-12-3, (d) FDU-12-4.

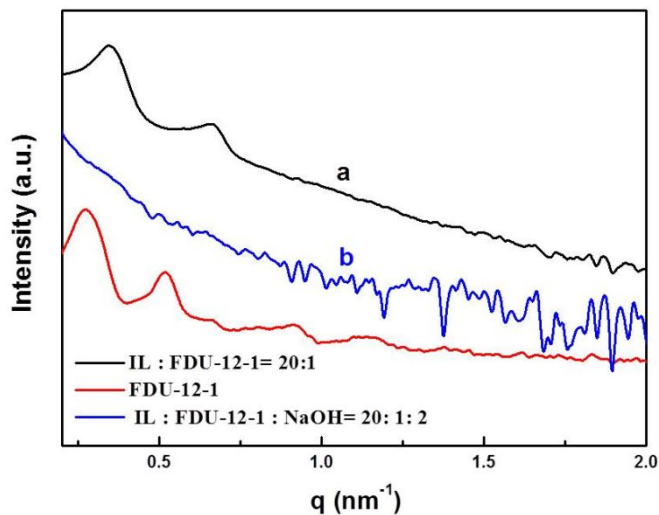


Figure S3. The stability of mesoporous structure of FDU-12-1 sample: (a) mass ratio of IL to FDU-12-1= 20 : 1, (b) mass ratio of IL : FDU-12-1 : NaOH= 20 : 1 : 2.

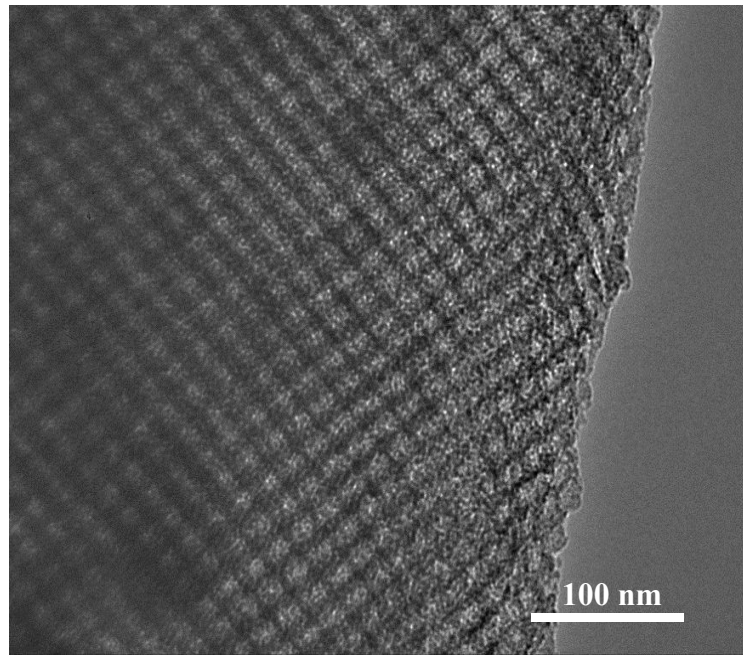


Figure S4. TEM image of the neat FDU-12-1 sample.

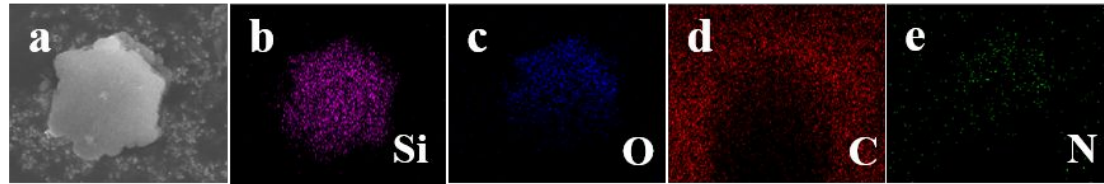


Figure S5. SEM images and the corresponding EDS elemental mapping images of the IL-FDU-12-1 sample prepared at $R = 1.5$.

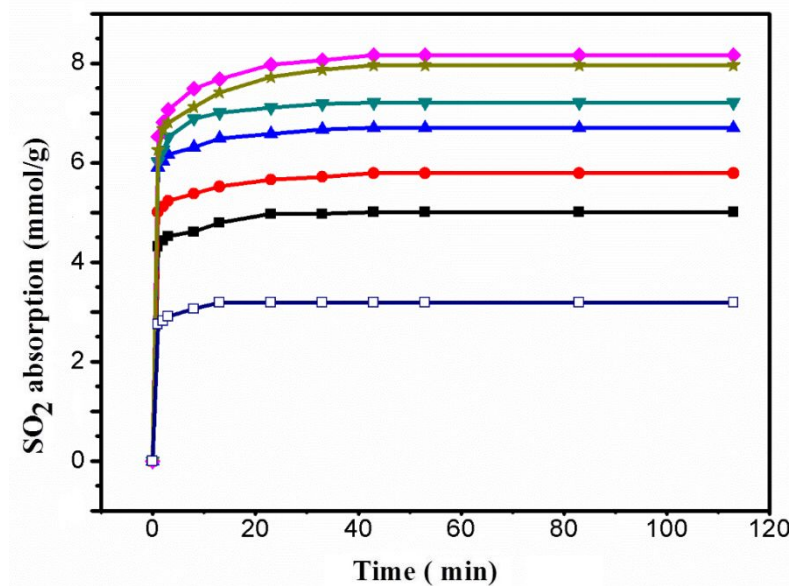


Figure S6. The effect of grafted IL content on SO_2 absorption capacity: -■-, no grafting; -●-, 0.23 mmol/g; -▲-, 0.33 mmol/g; -▼-, 0.40 mmol/g; -★-, 0.52 mmol/g; -◆-, 0.53 mmol/g; -□-, 0.15 mmol/g.

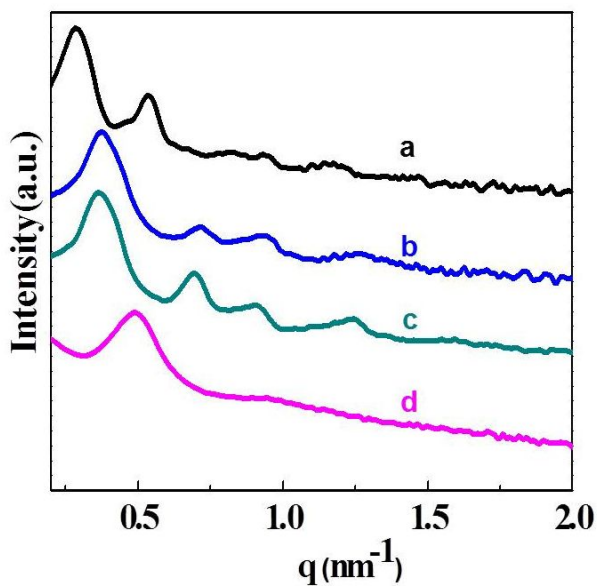
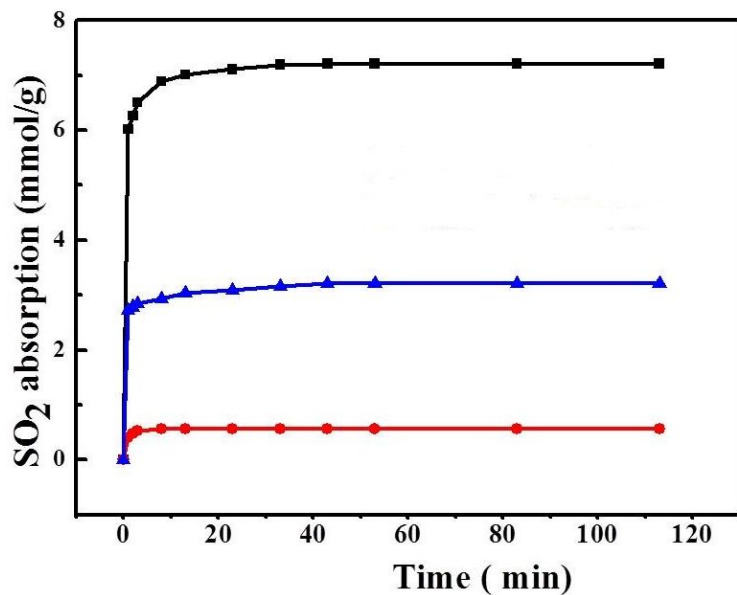
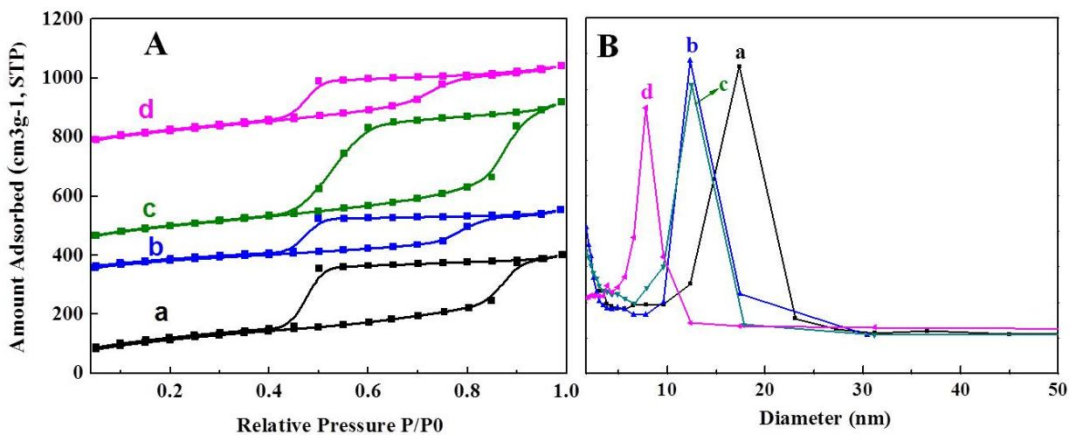


Figure S7. SAXS patterns of the IL@FDU-12 samples prepared at $R = 1.5$: (a), IL@FDU-12-1; (b), IL@FDU-12-2; (c), IL@FDU-12-3; (d), IL@FDU-12-4.



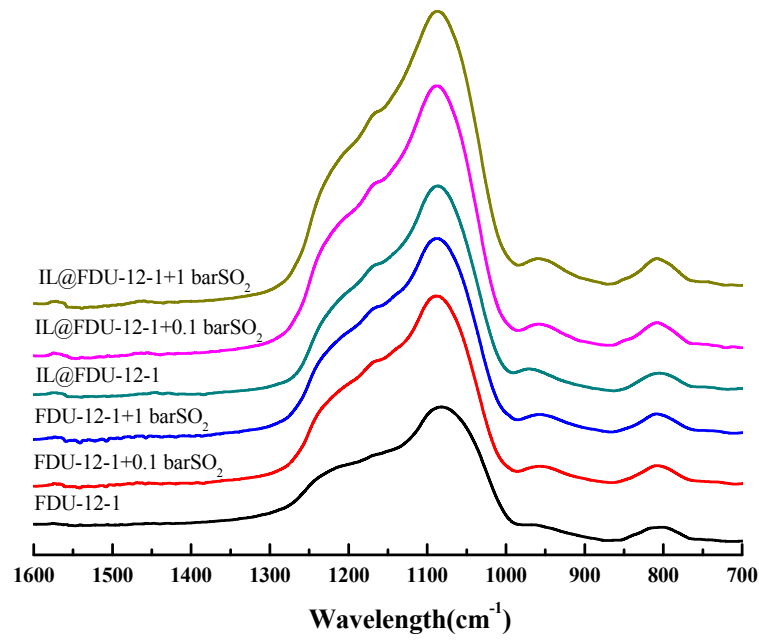


Figure S10. FT-IR spectra of FDU-12-1 and IL@FDU-12-1 synthesized at $R = 1.5$ before and after capture of SO_2 .

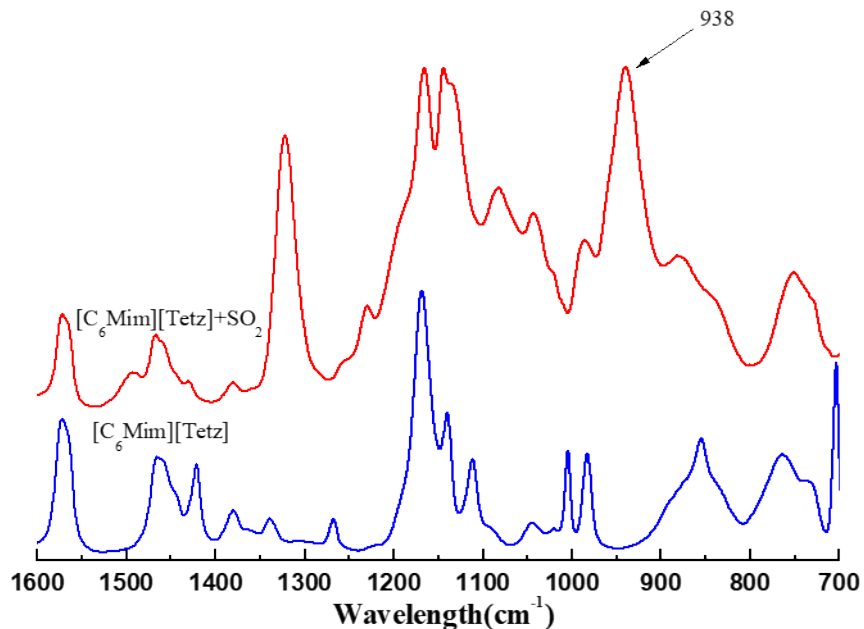


Figure S11. FT-IR spectra of the neat IL before and after capture of SO_2 .

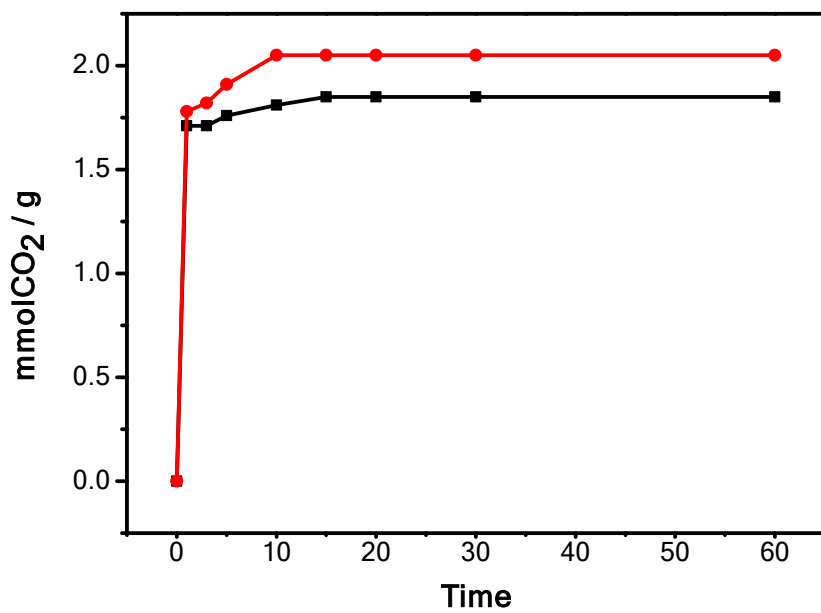


Figure S12. CO₂ uptake at 25 °C and 1 bar as a function of absorption time by IL@-FDU-12-1 synthesized at $R = 1.5$: -■-, neat FDU-12-1 and -●-, IL@-FDU-12-1.